

A Dynamic Nuclear Magnetic Resonance Study of Fluorine Exchange in Liquid Sulfur Tetrafluoride¹

Walter G. Klemperer,^{*2a} Jeanne K. Krieger, Michael D. McCreary,
E. L. Muetterties,^{*2b} Daniel D. Traficante, and George M. Whitesides^{*2c}

Contribution from the Departments of Chemistry, Massachusetts Institute of Technology, Cambridge, Massachusetts 02139, and Cornell University, Ithaca, New York 14850. Received April 7, 1975

Abstract: The temperature dependence of the NMR spectrum of SF₄ has been reexamined, and the observed line shapes in the region of intermediate exchange compared with theoretical line shapes calculated for a number of different methods of permuting axial and equatorial fluorine atoms. Carefully purified SF₄ yields experimental spectra in good agreement with those calculated assuming the intramolecular fluorine exchange characteristic of Berry pseudorotation; these experimental spectra do not closely resemble those calculated on the basis of any intermolecular permutation we have examined. The exchange rate in unpurified SF₄ is substantially higher than in carefully purified material. The line shapes observed for unpurified material can be matched to those calculated assuming permutations characteristic of several plausible bimolecular mechanisms; available data do not uniquely define the mechanism of this impurity-catalyzed exchange.

At low temperatures, liquid SF₄ displays an A₂B₂ NMR spectrum characteristic of a C_{2v} molecule,³ as the temperature is raised, fluorine site exchange leads to line broadening and eventual coalescence to a single sharp resonance.³ This spectral temperature dependence has been extensively examined, but a unique mechanistic interpretation of this dependence has proved elusive. In 1958, Cotton, George, and Waugh⁴ surmised that fluoride impurities induced fluorine exchange in their substantially contaminated samples. Muetterties and Phillips⁵ subsequently published similar spectra, and, noting a dependence of fluorine exchange rate on sample concentration, advocated intermolecular mechanisms involving dimeric or ionic intermediates. In a later publication,⁶ however, they emphasized the possibility that traces of HF might be catalyzing fluorine exchange and also expressed the belief that intramolecular exchange does occur, but at a rate lower than the observed higher-order processes. The hypothesis of impurity catalysis was supported by Bacon, Gillespie, and Quail,⁷ and more recently by Gibson, Abbott, and Janzen,⁸ who retarded the rate of fluorine exchange by careful sample purification. The latter authors, however, were unable to establish that all impurities had been removed.

Other physical studies of sulfur tetrafluoride have failed to clarify the relative importance of intra- and intermolecular paths for the fluorine exchange. Redington and coworkers strongly favored bimolecular mechanisms on the basis of matrix-isolation infrared spectra,^{9,10} and variations in NMR coupling constants and chemical shifts with medium have been interpreted as indicating intermolecular association of liquid SF₄.¹¹ Gas phase studies, employing both far-infrared spectroscopy¹² and electron diffraction,¹³ implicated intramolecular exchange processes. Theoretical studies^{14,15} also propose intramolecular exchange in the gas phase, thus lending credence to Muetterties and Phillips' hypothesis that intramolecular exchange might be observed in the liquid phase if higher-order processes could be suppressed.

The present dynamic NMR study was undertaken to delineate the site exchange scheme responsible for fluorine exchange in sulfur tetrafluoride, and thus unambiguously determine which, if any, of the proposed exchange mechanisms are consistent with experiments. The results of this investigation are reported in three parts: (i) generation of all possible site exchange schemes implied by intramolecular, impurity catalyzed, and bimolecular mechanisms,

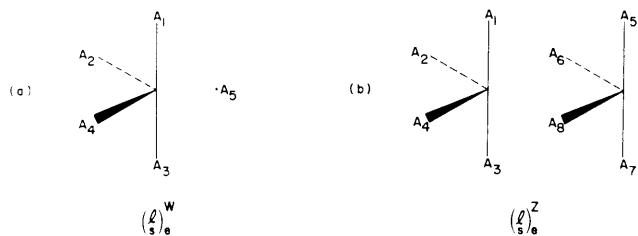


Figure 1. Labeling of the fluorine nuclei and sites in SF₄ and a fluoride impurity are defined by the reference configuration shown in (a). Fluorine nuclei and sites are labeled in (b) for bimolecular exchange processes.

which might imply different dependencies of NMR line shape on rate, (ii) simulation of rate dependent spectra based on these site exchange schemes, and (iii) comparison of the simulated spectra with experimental spectra of highly purified SF₄ samples as well as samples containing traces of HF. Interpretation of results indicates that both intramolecular and impurity catalyzed processes are operative in SF₄.

Site Exchange Schemes

Three classes of fluorine exchange mechanisms will be examined here: intramolecular exchange, exchange involving fluoride impurities, and bimolecular exchange. The general procedure for enumerating NMR differentiable reactions within each class has been presented in detail elsewhere;¹⁶ only results will be reported here. In brief, the $n!$ possible permutations of the n atoms involved in each mechanistic class are divided into sets of permutations (reactions), using symmetry arguments, such that reactions within each set, NMR nondifferentiable reactions, imply identical dependence of NMR line shape on rate. Then a single reaction is chosen from each set, thus forming a complete set of NMR differentiable reactions. The site exchange scheme implied by any mechanism within a given class may then be expressed in terms of combinations of reactions chosen from the appropriate complete set of NMR differentiable reactions.

There is an important symmetry argument that simplifies the analysis of processes. At the slow exchange limit, the A₂B₂ NMR spectrum of SF₄ is a symmetric spectrum in that the half of the spectrum due to axial fluorine resonances is the mirror image of the other half of the spectrum which is due to equatorial fluorine resonances. When exchange broadening sets in, the spectra may retain this symmetry or become asymmetric, i.e., lose mirror symmetry. Therefore, a site exchange scheme may be classified as either symmetric or asymmetric, depending on whether it implies symmetric or asymmetric spectra.¹⁷ A complete set of NMR differentiable reactions may accordingly be divided into two subsets, one containing symmetric reactions and the other containing asymmetric reactions. Asymmetric reactions will occur in conjugate pairs such that the entire spectrum implied by one member of a pair is the mirror image of the spectrum implied by the other member of the pair (see below).

Intramolecular Exchange. Since SF₄ contains four fluorine atoms, there exist 4! or 24 possible fluorine site permutations (reactions). Labeling atoms A₁–A₄ as in Figure 1a, it can be shown that the three reactions h₂^{ww}–h₄^{ww} listed in Table I form a complete set of NMR differentiable reactions. One of these, h₂^{ww}, implies no change of NMR line shape with rate. The remaining two are symmetric reactions. Consequently, any intramolecular exchange scheme must imply a symmetric NMR spectrum throughout the exchange region.

Table I. A Complete Set of NMR Differentiable Exchange Reactions for Intramolecular and Impurity Catalyzed Exchange Exchange in SF₄^a

*h ₂ ^{ww} = (24)ww	
h ₃ ^{ww} = (12)ww	
h ₄ ^{ww} = (12)(34)ww	
*h ₅ ^{ww} = (15)ww	*h ₇ ^{ww} = (25)ww
h ₆ ^{ww} = (15)(34)ww	h ₈ ^{ww} = (25)(34)ww
h ₉ ^{ww} = (345)ww	h ₁₀ ^{ww} = (354)ww = h ₉ ⁻¹ ww
h ₁₁ ^{ww} = (12)(345)ww	h ₁₂ ^{ww} = (12)(354)ww = h ₁₁ ⁻¹ ww

^aConjugate pairs of asymmetric reactions have been written on the same line, and reactions which imply more than one resonance in the fast exchange limit have been starred.

Table II. A Complete Set of NMR Differentiable Reactions Which Involve Bimolecular Exchange of Only One Fluorine Atom from Each SF₄ Molecule^a

h ₁ ^{zz} = (47)zz	
*h ₂ ^{zz} = (37)zz	*h ₃ ^{zz} = (48)zz
h ₄ ^{zz} = (12)(47)zz	h ₅ ^{zz} = (12)(38)zz
h ₆ ^{zz} = (12)(37)zz	h ₇ ^{zz} = (12)(48)zz
h ₈ ^{zz} = (12)(47)(56)zz	
h ₉ ^{zz} = (12)(37)(56)zz	h ₁₀ ^{zz} = (12)(48)(56)zz
[h ₁₁ ^{zz} = (347)zz	[h ₁₄ ^{zz} = (384)zz
[h ₁₂ ^{zz} = (374)zz	[h ₁₃ ^{zz} = (348)zz
[h ₁₅ ^{zz} = (12)(347)zz	[h ₂₀ ^{zz} = (12)(384)zz
[h ₁₆ ^{zz} = (12)(374)zz	[h ₁₉ ^{zz} = (12)(348)zz
[h ₁₇ ^{zz} = (12)(478)zz	[h ₂₂ ^{zz} = (12)(387)zz
[h ₁₈ ^{zz} = (12)(487)zz	[h ₂₁ ^{zz} = (12)(378)zz
[h ₂₃ ^{zz} = (12)(347)(56)zz	[h ₂₆ ^{zz} = (12)(384)(56)zz
[h ₂₄ ^{zz} = (12)(374)(56)zz	[h ₂₅ ^{zz} = (12)(348)(56)zz
[h ₂₇ ^{zz} = (3478)zz	
[h ₂₈ ^{zz} = (3874)zz	
h ₂₉ ^{zz} = (3487)zz	
[h ₃₀ ^{zz} = (12)(3478)zz	
[h ₃₁ ^{zz} = (12)(3874)zz	
[h ₃₂ ^{zz} = (12)(3487)zz	
[h ₃₃ ^{zz} = (12)(3784)zz	
[h ₃₄ ^{zz} = (12)(3478)(56)zz	
[h ₃₅ ^{zz} = (12)(3874)(56)zz	
h ₃₆ ^{zz} = (12)(3487)(56)zz	

^aConjugate pairs of asymmetric reactions have been written on the same line, pairs of reactions related as reaction and reverse reaction are enclosed by brackets, and reactions which imply more than one resonance in the fast exchange limit have been starred.

Exchange Involving Fluoride Impurities. When fluorine impurities are involved in an exchange process, five fluorine atoms, labeled A₁–A₅ in Figure 1a, must be taken into account. Species A₅ may be the fluorine atom in HF, an F⁻ ion from self-ionization of SF₄, or any other fluoride impurity. The set of 5! = 120 possible site permutations contains 11 NMR differentiable reactions, eight of which involve participation of A₅ in the exchange process. These reactions, h₅^{ww}–h₁₂^{ww}, are presented in Table I. Each of them is an asymmetric reaction, but members of two of the conjugate pairs are related as reaction and reverse reaction and must therefore occur with equal probability (microscopic reversibility). Thus each of these two pairs represents a single process which implies symmetric spectra.

Bimolecular Exchange. Bimolecular mechanisms involve eight atoms, labeled A₁–A₈ in Figure 1b. Eighty-two of the 8! = 40320 possible site permutations may be chosen to form a complete set of NMR differentiable reactions. If one ignores those reactions which involve only intramolecular exchange, and further ignores those reactions which involve transfer of more than one fluorine atom from one sulfur atom to the other, only 36 NMR differentiable reactions remain. These reactions are listed in Table II.

Results and Discussion

Figure 3 illustrates the temperature dependence observed for purified liquid, SF₄ at 9.2 MHz. Low values of the H₀



Figure 2. Schematic slow-exchange spectrum of SF₄.

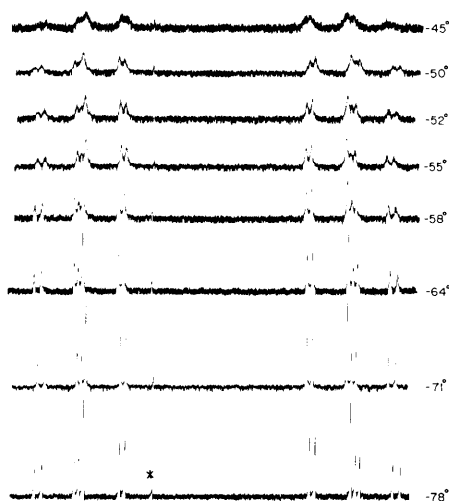


Figure 3. Temperature-dependent ¹⁹F NMR spectra of purified liquid SF₄ (9.2 MHz). The peak indicated by an asterisk is SOF₂ present as an impurity. These spectra were not taken with a frequency-locked spectrometer, and small apparent variations in chemical shift are not significant. Certain details of the apparent intensities of lines 6 and 7 close to the slow-exchange limit are artifacts; see the text for a discussion.

field were used in these experiments to introduce as much second-order character into the spectrum as possible. The line shapes of these low-field spectra were much more sensitive to mechanism than were those at higher field, both because the relatively large value of $J_{ac}/\delta\nu$ resulted in large differences in the broadening of the individual lines in the intermediate exchange region and because the increased separations between the components of the multiplets at low field made these differences more easily observable experimentally. Careful attention to the amplitude of the H₁ field was required to avoid saturating these spectra, particularly close to the slow exchange limit. The form of the spectra was not altered when Ph₃P=NC₆H₄F was included in the purified sample as a fluoride scavenger. To simplify discussion the spectral lines will be referenced as indicated in Figure 2. Two spectral features are important in mechanistic distinctions. First, the experimental spectra are symmetrical with the broadening of each line in the multiplet of lines 1-7 mirrored by the broadening of the symmetrically disposed line in the multiplet of lines 8-14. Second, groups of lines are characterized by well-defined differential broadenings: line 7 broadens more rapidly than line 6, line 4 broadens more rapidly than line 3, and line 1 broadens more rapidly than line 2, as the sample temperature is raised. Note that this relative line broadening is only clearly visible in the spectra of Figure 3 at temperatures above -64°. The apparent relative peaks observed in the spectra at -71 and -64° (particularly, the apparently greater height of line 7 relative to line 6) are artifacts, reflecting saturation and transient instrument response. The differential broadenings of the lines in these multiplets form the basis for the most important of the mechanistic distinctions that follow.

Spectra taken of unpurified SF₄ under similar conditions are qualitatively different in several respects (Figure 4). In the intermediate exchange region the spectra show a subtle

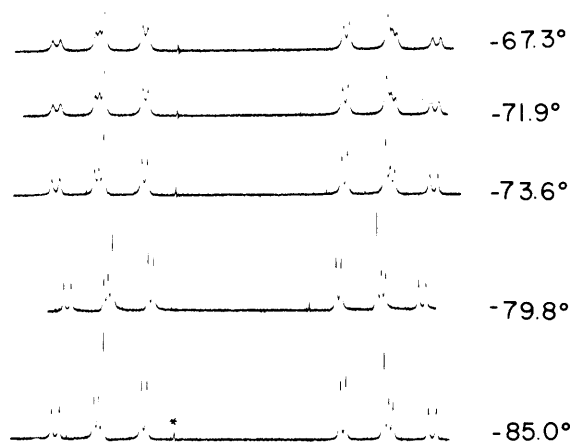


Figure 4. Temperature-dependent ¹⁹F NMR spectra of unpurified liquid SF₄ (9.2 MHz). The direction of scan of the spectrum at -80° is reversed from that of the other spectra (note the position of the SOF₂ peak, marked with an asterisk).

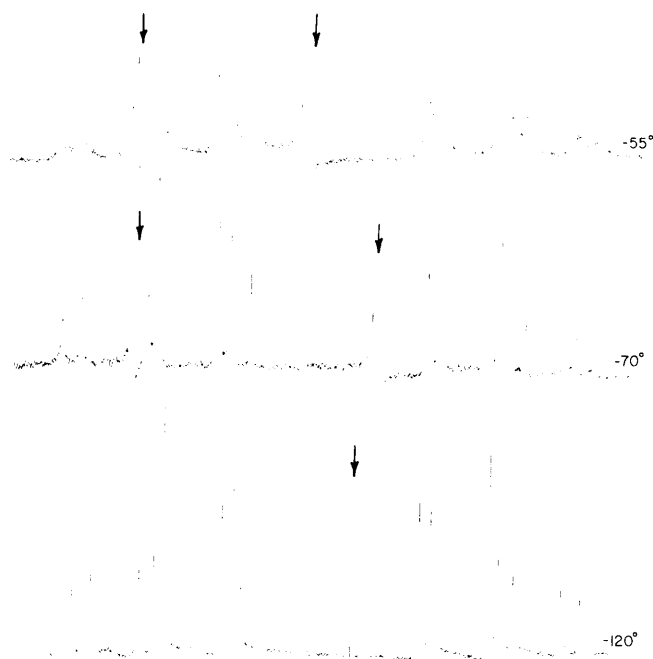


Figure 5. Temperature-dependent ¹⁹F NMR spectra of purified SF₄ in 1-butene solution (12% v:v) at 6.5 MHz. The features indicated by arrows are artifacts, resulting from fold-over in the Fourier transform.

but real asymmetry. Especially notable are the differences in the peak-to-valley ratio for the 6,7 and 8,9 transitions, and in the shapes of 3,4,5 and 10,11,12 multiplets at -67°. A critical distinction is the absence of one of the differential line broadenings, characteristic of the spectra of pure SF₄, in the impure sample; the 3 and 4 transitions in the impure sample seem to broaden approximately equally as the sample temperature is increased. Finally, there is a differential in absolute exchange rate since a corresponding degree of line broadening for the unpurified sample occurs at significantly lower temperature than for the purified sample. The line broadening of the 6,7 and 8,9 multiplets, judged by the peak-to-valley ratio, correspond for spectra of the purified sample at -50° and the unpurified sample at -72°.

Dilution of the sample has no significant influence on the temperature dependence of the spectra of the purified SF₄. Figure 5 shows several spectra taken of a solution of SF₄ in 1-butene (12% v:v SF₄:butene). Although these spectra were taken at 6.5 MHz, and are thus not directly comparable to those shown in Figure 3, it is clear that the line

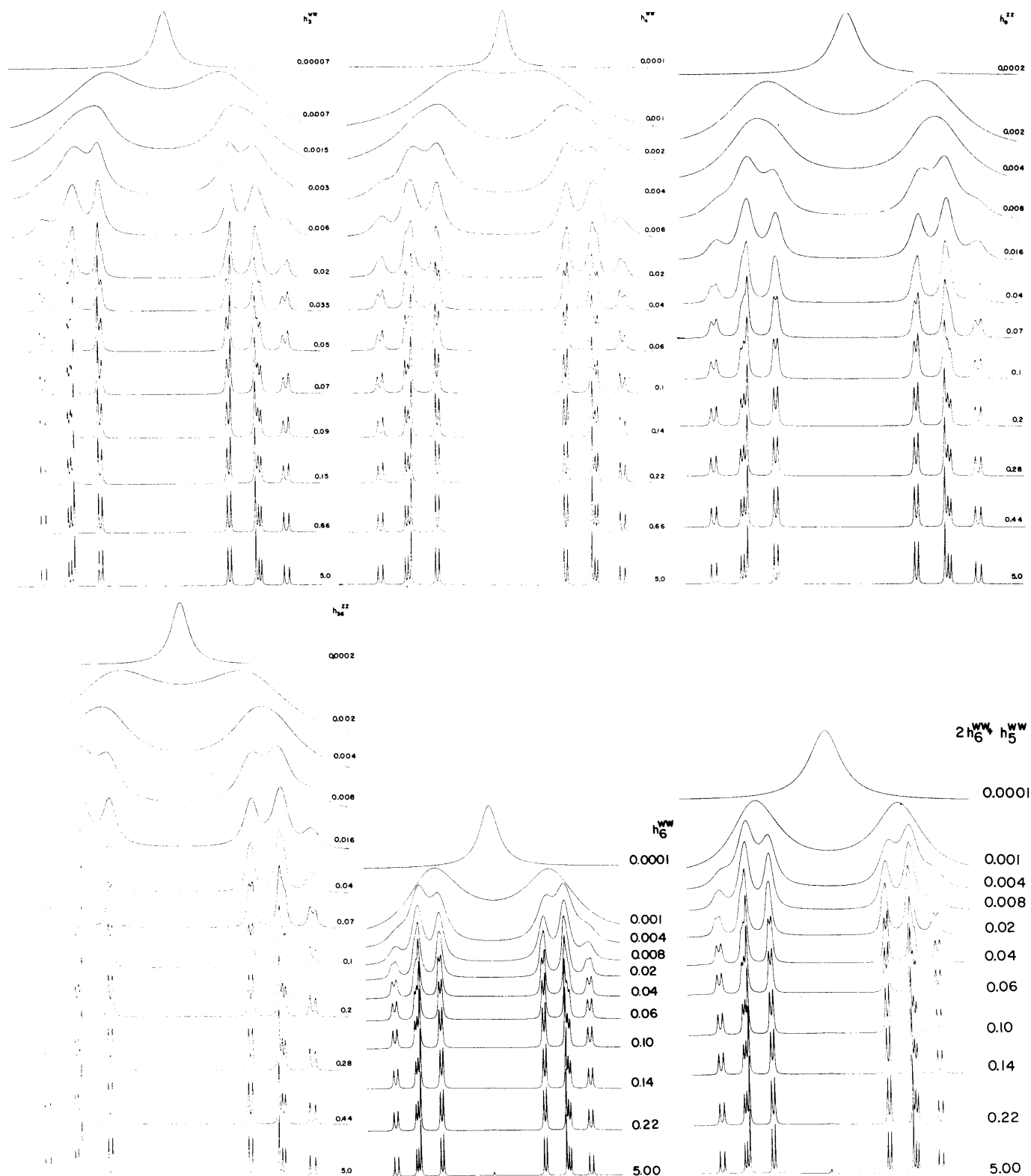


Figure 6. Spectra calculated for the permutations h_3^{ww} , h_4^{ww} , h_6^{ww} , h_9^{zz} , h_{36}^{zz} , and $(h_5^{ww} + 2h_6^{ww})$ as a function of the preexchange lifetime, τ (sec). As a result of changes in the program τ is defined differently for the series h_n^{ww} and h_m^{zz} ; τ for the latter group should be divided by two to be consistent with the definition used for the former. The line in the center of the spectra for $h_5^{ww} + 2h_6^{ww}$ is fluoride. For mechanisms h_6^{ww} and $2h_6^{ww} + h_5^{ww}$, τ refers to τ_{SF_4} .

broadenings characterizing the two sets of spectra at -55° are comparable. These spectra and those shown in Figure 3 were taken in different laboratories using samples purified by different procedures; the good agreement between the differential line broadenings characterizing these two sets of spectra indicates the reproducibility of these features.

These experimental spectra were compared with theoretical simulations derived from the NMR-differentiable per-

mutations listed in Tables I and II (Figures 6 and 7). The procedures used to carry out these simulations are described in a following section. Only seven permutations (or combinations of permutations) corresponding to mechanisms that seemed particularly plausible, or that had previously been explicitly postulated in the literature, were calculated over a full range of preexchange lifetimes; the remainder were examined only at two representative exchange rates in the in-

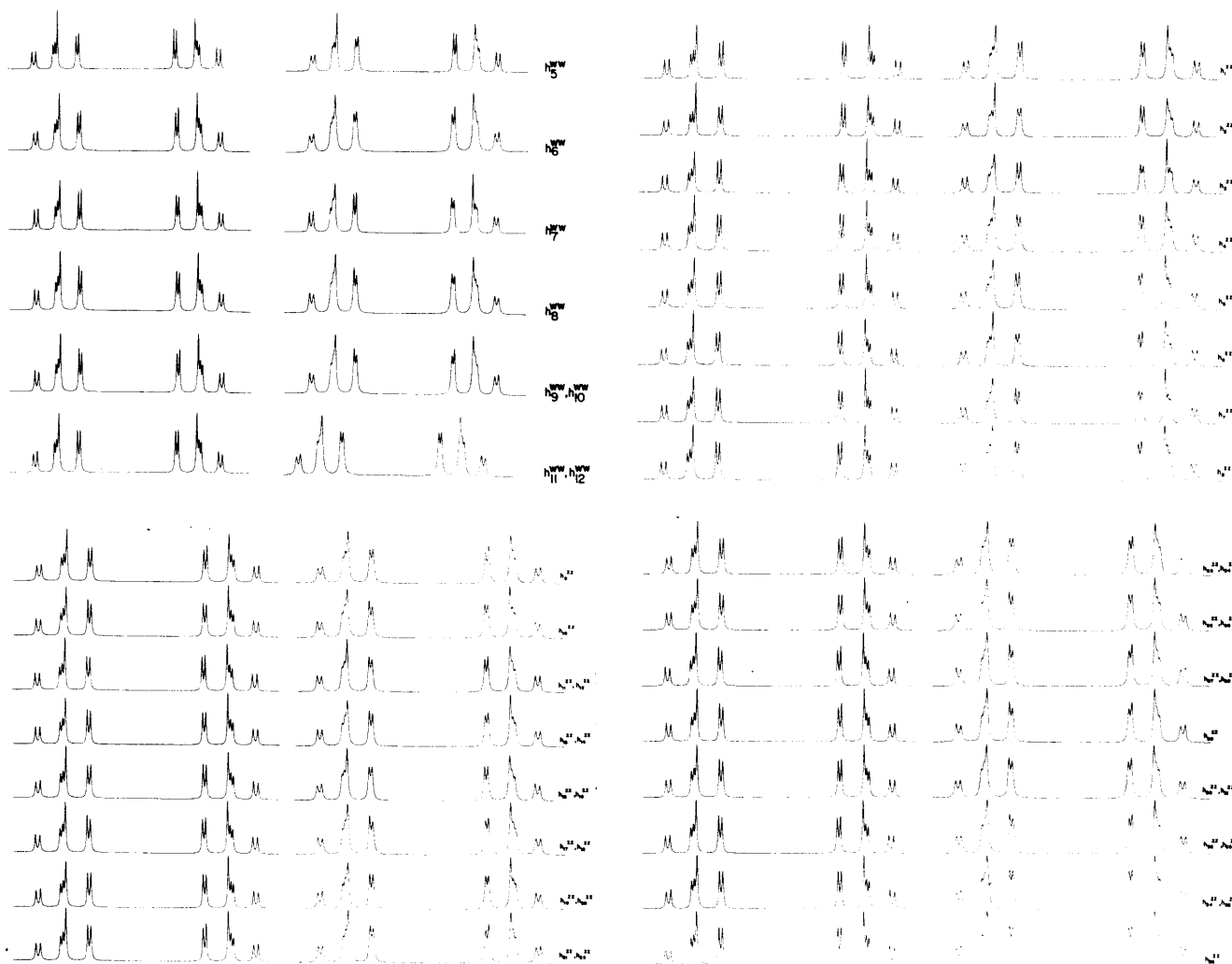
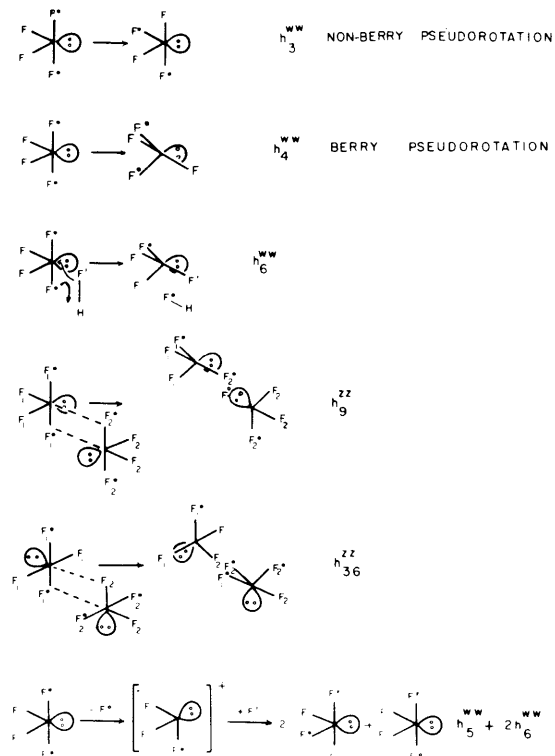


Figure 7. Spectra calculated for a variety of permutations in the intermediate exchange region. For each permutation two values of τ were used: the left-hand spectrum for each was calculated for $\tau_{\text{SF}_4} = 0.1$ sec; for the right-hand spectrum, $\tau_{\text{SF}_4} = 0.05$ sec. The line in the center of the spectra for $h_5^{\text{ww}}-h_{12}^{\text{ww}}$ is fluoride. For these spectra, $[\text{F}^-]/[\text{SF}_4] = 0.05$.

intermediate exchange region. The two intramolecular exchanges, h_3^{ww} and h_4^{ww} , are the permutations that characterize non-Berry and Berry pseudorotations, respectively. Plausible bimolecular mechanisms involving SF_4 and fluoride ion (h_6^{ww}) or two SF_4 molecules (h_9^{zz} and h_{36}^{zz}) and a dissociative mechanism ($h_5^{\text{ww}} + 2h_6^{\text{ww}}$) were also calculated (Scheme I). Many other possible permutations could, of course, also be rationalized in terms of plausible mechanisms.

Remarkably and fortunately, only one of the possible permutations generates spectra in satisfactory agreement with the experimental spectra of purified SF_4 , viz., h_4^{ww} , the permutation corresponding to the intramolecular Berry pseudorotation. A number of features of the experimental and calculated line shapes can be used to identify h_4^{ww} as the permutation characterizing the experimental spectrum. The most distinctive is the differential broadening of lines 3 and 4 (or, symmetrically, of lines 11 and 12). Only in the experimental spectra and in the calculated spectra based on h_4^{ww} does line 4 broaden more rapidly than line 3; in all other permutations, either line 3 broadens more rapidly than line 4 or they broaden at comparable rates. We conclude that the process responsible for averaging the chemical shifts of carefully purified SF_4 (pure liquid or in butene solution) is an intramolecular rearrangement that has the ligand atom permutational character expected for the intramolecular Berry pseudorotation. This conclusion receives independent support from the observation that this ex-

Scheme I. Axial-Equatorial Interchange Mechanisms



change reaction is sensibly independent of the concentration of SF₄, and to a change in medium from pure SF₄ to butene-SF₄.

The mechanism responsible for the averaging of the axial and equatorial fluorine chemical shifts of SF₄ in unpurified samples appears to be different than that in purified samples. Exchange occurs more rapidly in unpurified than in purified samples and is characterized by line shapes in the intermediate exchange region that are appreciably different than those of the purified samples. The presently available data are not sufficient to permit clear delineation of the dominant mechanism (or mechanisms) for exchange in the unpurified samples. The asymmetry between the upfield and downfield multiplets of the experimental spectra (Figure 2) is compatible with any of several types of associative and dissociative mechanisms. The chemical species SF₃⁺,¹⁸ SF₅⁻,¹⁹ and HF₂⁻²⁰ are all well-known and could provide plausible intermediates in such reactions. Without more information on the influence of solution variables on this (presumably impurity-catalyzed) exchange, it is not profitable to speculate further about its mechanism.

In summary, the data in this paper establish that pure SF₄ interchanges axial and equatorial fluorines by an intramolecular process having the permutational character of a Berry pseudorotation. Fluorine interchange in impure solutions appears to proceed predominantly through a rapid, impurity-catalyzed reaction of unspecified character.²¹

Experimental Section

Preparation of SF₄ Samples. Two different sample preparation protocols were developed. Samples used at M.I.T. for 6.5-MHz fluorine spectra were purified by the following procedure. Crude SF₄ (Peninsular Chemresearch, Inc.) was distilled into one bulb of a dry Pyrex high-vacuum line equipped with unlubricated Teflon stopcocks. This bulb contained a small quantity of sodium fluoride that had been dried on the line at ca. 250° and 0.001 Torr. The SF₄ was distilled from this bulb through traps held at -83° and -97°, and condensed into a second sodium fluoride-containing trap, held at -180°. The sample in this trap was allowed to warm until it became liquid, let stand for 30 min, and distilled into a dried, thick-walled, 10-mm Pyrex NMR tube. The tube was cooled to -180° and was then sealed under vacuum with care not to pyrolyze the sample during the sealing procedure. Certain samples were distilled into NMR tubes containing previously degassed 1-butene in order to test the influence of SF₄ concentration on fluorine exchange rates.

Samples used at duPont for 9.2-MHz fluorine spectra were prepared following a different procedure. Crude SF₄, prepared from SCl₂ and NaF (acetonitrile), was purified by distillation at 1 atm and was then stored in a stainless steel cylinder. The steel cylinder was then attached to an all-quartz vacuum line. NMR samples were prepared by first distilling SF₄ from the cylinder into a flask on the flamed out vacuum line which contained triphenylphosphine(*p*-fluorophenyl)imine as a fluoride scavenger and a Teflon-coated magnetic stirring bar.²² The SF₄ was stirred over this scavenger for 45 min at Dry Ice-acetone temperature and then subjected to two bulb-to-bulb distillations before being transferred to a quartz NMR tube and the tube was sealed. Some NMR samples were prepared that contained a crystal of triphenylphosphine(*p*-fluorophenyl)imine in the NMR tube; others did not contain this scavenger.

NMR Spectral Measurements. ¹⁹F spectra at M.I.T. were taken with a Bruker HFX-90 spectrometer, modified to operate at 6.5000 MHz. Spectra were taken in Fourier transform mode using Digilab Models FTS/NMR-3 data system and a Perkin-Elmer Model 209 A RF amplifier modified for pulsed NMR applications. A Bruker variable temperature accessory was used with a thermocouple positioned 0.5 cm below the bottom of the NMR tube. The thermocouple was calibrated in place against a pentane thermometer.

Spectra at duPont were taken on a Varian HR-60 spectrometer, with a Varian variable temperature accessory, modified to operate at 9.2 MHz.

Computational Procedures

Site Exchange Schemes. Complete sets of NMR differentiable reactions for the intramolecular case and the case involving a fluoride impurity were generated using combinatorial aids reviewed elsewhere.¹⁶ The complexity of the bimolecular case necessitated the use of a computer. Generation of a complete set of NMR differentiable reactions for the bimolecular case, i.e., generation of a complete set of double coset representatives¹⁶ in S₈ with respect to the subgroup S₂ [S₂ + S₂] was accomplished by computer generating each double coset, printing out one member of each, but storing all the members of each double coset in coded form using Marshall Hall's Method of Derangements.²³ The completeness of the set of coset representatives was assured when all 40320 permutations in S₈ had been stored (in coded form). This approach proved to be reasonably efficient, the program requiring less than 150 K bytes of the CPU and under 2 min time on an IBM 360/65.

Spectral Simulations. Spectra corresponding to intramolecular exchange schemes were obtained in the representation of eigenfunctions of the slow-exchange Hamiltonian using standard density matrix procedures,²⁴⁻²⁷ and solving eq 1.

$$I(\omega) \propto \text{Re}[\mathbf{I}^+ \cdot \mathbf{A}^{-1} \cdot \mathbf{I}^{+'}] \quad (1)$$

Here, $I(\omega)$ is the spectral intensity as a function of frequency, ω , \mathbf{A} is defined as previously,²⁵ and $\mathbf{I}^+ = \mathbf{I}^{+'}$ is a vector consisting of matrix elements of the raising operator between eigenfunctions of the nuclear spin Hamiltonian giving rise to the lines involved in the exchange.²⁸ For problems involving *intermolecular* exchange, in which the concentration of species A [\mathbf{A}] is not equivalent to the concentration of species B [\mathbf{B}], the elements of $\mathbf{I}^{+'}$ contain correction terms for the relative concentration of the two species. The elements of $\mathbf{I}^{+'}$ and \mathbf{I}^+ are related by the expression $\mathbf{I}_A^{+'} = \mathbf{I}_A^+ [\mathbf{A}] / [\mathbf{B}]$. Intermolecular exchange schemes were simulated using related methods outlined by Kaplan and Alexander.²⁶

In this treatment the exchange process is envisioned to occur within a collision complex that is sufficiently short-lived that its existence does not directly influence the spectra of the components, but simply serves as a vehicle to permit exchange of nuclei. This exchange process is treated by a procedure analogous to that for intramolecular exchanges by considering the influence of permuting nuclear spins on the density matrices of the components. Since the collision complex is assumed to be so short-lived that the detailed forms of its nuclear spin Hamiltonian and wave functions are not important, a wave function suitable for the problem is assumed for convenience to be that obtained simply by multiplying the wave functions of the two colliding components. This assumption is equivalent to a physical picture of the collision complex in which there is no interaction between the colliding components or, equivalently, to one in which the perturbation of the Hamiltonians of the colliding components resulting for the collision is so short-lived that the nuclear spin systems do not respond appreciably. Thus, if the eigenfunctions ψ_A and ψ_B of the respective slow-exchange Hamiltonians \mathcal{H}_A and \mathcal{H}_B of the reacting molecules A and B are expressed in matrix form in terms of suitable basis sets of simple nuclear spin product functions ϕ_A and ϕ_B by eq 2, the corresponding functions for the collision complex are given by cross products of the matrices for A and B, and the "density matrix" of the collision complex by the cross product of the density matrices of A and B (eq 5).

$$\psi_A = \mathcal{H}_A \phi_A \quad (2a)$$

$$\psi_B = \mathcal{H}_B \phi_B \quad (2b)$$

$$\phi_{AB} = \phi_A \times \phi_B \quad (3)$$

$$\mathcal{H}_{AB} = \mathcal{H}_A \times \mathcal{H}_B \quad (4)$$

$$\rho_{AB} = \rho_A \times \rho_B \quad (5)$$

The quantity required in this formalism for the calculation of the influence of the exchange process on the line shapes is the time derivative of the density matrix, viz., for molecule A, eq 6.

$$\left(\frac{\partial \rho_A}{\partial t}\right)_{\text{exchange}} = \frac{1}{\tau_A} [\rho_A^{\text{after}} - \rho_A^{\text{before}}] \quad (6)$$

In this equation the superscripts "after" and "before" have their usual meaning of "after exchange" and "before exchange", and τ_A is the mean preexchange lifetime of species A.

For the problems in which the concentration of species A is not equal to the concentration of species B, the ratio of the mean preexchange lifetimes of species A and B is given by $\tau_A/\tau_B = [A]/[B]$. The permutation of nuclear spins in the collision complex can be summarized by eq 7, and the influence of this permutation on the wave function ψ_{AB} for the collision complex by eq 8

$$\phi_{AB}^{\text{after}} = \mathbf{X}\phi_{AB}^{\text{before}} \quad (7)$$

$$\psi_{AB}^{\text{after}} = \mathcal{H}_{AB} \mathbf{X} \mathcal{H}_{AB}^{-1} \psi_{AB}^{\text{before}} = \mathbf{R}\psi_{AB}^{\text{before}} \quad (8)$$

The term ρ_A^{after} in eq 6 is evaluated by separating ρ_{AB}^{after} (eq 9) into the terms for the isolated molecule of A by averaging corresponding elements of ρ_{AB} that contain elements diagonal in ρ_B (eq 10);²⁶ in the latter equation, e.g., $\text{Tr}\rho_B$ is the trace of ρ_B .

$$\rho_{AB}^{\text{after}} = \mathbf{R}\rho_{AB}^{\text{before}}\mathbf{R}^{-1} = \mathbf{R}(\rho_A^{\text{before}} \times \rho_B^{\text{before}})\mathbf{R}^{-1} \quad (9)$$

$$\rho_A^{\text{after}} = \text{Tr}_B(\mathbf{R}\rho_{AB}^{\text{before}}\mathbf{R}^{-1})/\text{Tr}\rho_B \quad (10)$$

Equation 10 can be combined with eq 6 and expanded to yield the elements of the kinetic exchange matrix \mathbf{K}^{25} (eq 11). Four types of elements make up this matrix: those describing transfer of magnetization between the lines of molecule A, K_{mn} ; those describing transfer from lines of A to lines of B, $K_{m\nu}$; those from B to A, $K_{\mu n}$; and those among the lines of B, $K_{\mu\nu}$. In these equations Roman indices refer to molecule A, and Greek indices to molecule B. The subscripts of the elements of ρ and R refer to eigenfunctions; those of K refer to lines. Thus, in eq 11b, $K_{m\nu}$ is the rate constant for transfer of magnetization between line m (the transition between ψ_i and ψ_j of molecule A) and line ν (the transition between ψ_γ and ψ_ϵ of molecule B). The term $\rho_{\gamma\epsilon} = (\psi_\gamma | \rho | \psi_\epsilon)$ is an element of ρ_B ; the term

$$\rho_{ij,\gamma\epsilon} = (\psi_i | \rho | \psi_j)(\psi_\gamma | \rho | \psi_\epsilon)$$

is an element of ρ_{AB} . N_A and N_B are normalization constants derived from $\text{Tr}\rho_A$ and $\text{Tr}\rho_B$, and numerically equal to the dimensions of ρ_A and ρ_B , respectively. (That is, to the number of states defined by the respective slow-exchange Hamiltonians, \mathcal{H}_A and \mathcal{H}_B . The ratio N_A/N_B is equivalent to the total observed intensities of species A relative to species B, if both species are present in equal concentration.) The Kronecker delta is δ .

$$\left(\frac{K_{mn}}{\tau_A} = \frac{\partial \rho_{ij,kl}}{\partial t}\right)_{\text{exch}} = \frac{1}{\tau_A} \left[\sum_{\alpha,\beta} \frac{N_B}{N_A} \frac{R_{i\alpha,k\beta} R_{j\alpha,l\beta} \rho_{kl}}{N_B} - \delta_{ik} \delta_{jl} \rho_{kl} \right] \quad (11a)$$

$$\left(\frac{K_{m\nu}}{\tau_A} = \frac{\partial \rho_{ij,\gamma\epsilon}}{\partial t}\right)_{\text{exch}} = \frac{1}{\tau_A} \left[\sum_{\alpha} \frac{N_B}{N_A} \sum_k \frac{R_{i\alpha,k\gamma} R_{j\alpha,k\epsilon} \rho_{\gamma\epsilon}}{N_B} \right] \quad (11b)$$

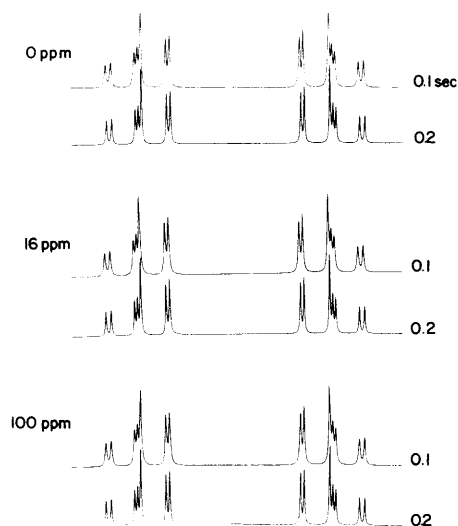


Figure 8. The influence of the chemical shift differences between fluoride ion and the fluorines of SF_4 on line shapes in the intermediate exchange region for h_9^{w} is small. Spectra were simulated assuming $[F^-]/[\text{SF}_4] = 0.05$ ($\tau = \tau_{\text{SF}_4}$).

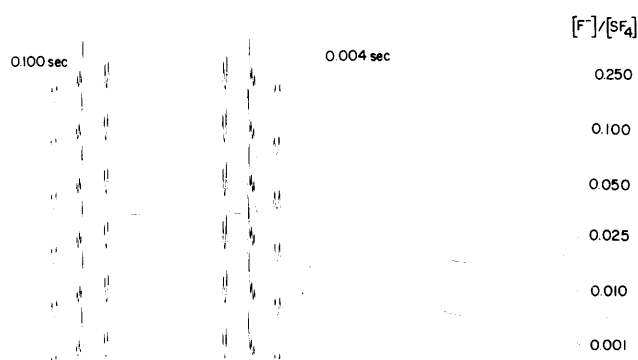


Figure 9. Spectra calculated at two values of τ_{SF_4} for h_6^{w} , at several relative concentrations of F^- and SF_4 .

$$\left(\frac{K_{\mu n}}{\tau_B} = \frac{\partial \rho_{\alpha\beta,kl}}{\partial t}\right)_{\text{exch}} = \frac{1}{\tau_B} \left[\sum_i \frac{N_A}{N_B} \sum_\gamma \frac{R_{i\alpha,k\gamma} R_{i\beta,l\gamma} \rho_{kl}}{N_A} \right] \quad (11c)$$

$$\left(\frac{K_{\mu\nu}}{\tau_B} = \frac{\partial \rho_{\alpha\beta,\gamma\epsilon}}{\partial t}\right)_{\text{exch}} = \frac{1}{\tau_B} \left[\sum_{i,k} \frac{N_A}{N_A} \frac{R_{i\alpha,k\gamma} R_{i\beta,k\epsilon} \rho_{\gamma\epsilon}}{N_A} - \delta_{\alpha\gamma} \delta_{\beta\epsilon} \rho_{\gamma\epsilon} \right] \quad (11d)$$

Equations 11a-d are specific for problems involving mutual exchange, viz., nuclear permutation schemes in which the reverse process is indistinguishable from the forward process ($R = R^{-1}$; h_4^{zz} , h_9^{zz}). For problems involving non-mutual exchange (n.m. exch)—that is, for any elementary process that is not microscopically reversible (e.g., h_9^{w})—a related equation that explicitly evaluates both forward and reverse reactions must be used (e.g., eq 12)²⁹

$$\left(\frac{\partial \rho_A}{\partial t}\right)_{\text{n.m. exch}} = \frac{1}{2\tau} \left[\frac{\text{Tr}_B(\mathbf{R}\rho_A \times \rho_B \mathbf{R}^{-1} + \mathbf{R}^{-1}\rho_A \times \rho_B \mathbf{R})}{\text{Tr}\rho_B} - 2\rho_A \right] \quad (12a)$$

$$\left(\frac{\partial \rho_B}{\partial t}\right)_{\text{n.m. exch}} = \frac{1}{2\tau} \left[\frac{\text{Tr}_A(\mathbf{R}\rho_A \times \rho_B \mathbf{R}^{-1} + \mathbf{R}^{-1}\rho_A \times \rho_B \mathbf{R})}{\text{Tr}\rho_A} - 2\rho_B \right] \quad (12b)$$

Use of the relationship between the transpose and inverse of $\mathbf{R}, \mathbf{R}^t = \mathbf{R}^{-1}$, permits facile evaluation of eq 12 by summation of diagonal elements of \mathbf{K} and use of a symmetrical form of \mathbf{K} even for problems involving nonmutual exchange (eq 13); these equations essentially average symmetrical exchange paths that are not individually microscopically reversible.

$$(K_{mn})_{n.m. \text{ exch}} = (K_{nm})_{n.m. \text{ exch}} = [K_{mn} + K_{nm}]/2 \quad (13a)$$

$$(K_{\mu\nu})_{n.m. \text{ exch}} = (K_{\nu\mu})_{n.m. \text{ exch}} = [K_{\mu\nu} + K_{\nu\mu}]/2 \quad (13b)$$

$$(K_{\mu n})_{n.m. \text{ exch}} = (K_{n\mu})_{n.m. \text{ exch}} = [(N_B/N_A)K_{n\mu} + (N_A/N_B)K_{\mu n}]/2 \quad (13c)$$

The \mathbf{K} matrices assembled from these equations were used in the programs described previously for spectral simulation.^{24,25} The magnetic parameters used in the calculations were: at 9.2 MHz (in Hz), $\delta\nu = 478.8$, $J_{a,c} = 76.3$; $J_{e,c} = 100.0$; $J_{a,e} = 50.0$. For simulations of mechanisms involving exchange between SF_4 and fluoride ion, the chemical shift of the fluoride was routinely set equal to the average of ν_a and ν_e . At the concentrations used to stimulate these spectra, $[\text{F}^-]/[\text{SF}_4] = 0.05$, the chemical shift difference between the fluoride and the fluorine of SF_4 has no influence on the shape of the calculated spectra (Figure 8). The relative signs of the fluorine-fluorine coupling constants did not influence the spectra.

Several spectra were calculated for h_6^{ww} to check whether the qualitative features of the line shapes used to discard this and related fluoride-catalyzed exchange processes depended on the ratio $[\text{F}^-]/[\text{SF}_4]$.³⁰ Figure 9 summarizes these spectra. Even at the lowest ratio tried ($[\text{F}^-]/[\text{SF}_4] = 0.001$), the spectra retain a pronounced asymmetry and are easily distinguishable from those observed experimentally. We conclude from these calculations that the central conclusion from this work—that an intramolecular, Berry, pseudorotation is responsible for fluorine interchange in purified SF_4 —is independent of the particular F^- concentration assumed in calculating fluoride-catalyzed exchange pathways.

Acknowledgments. Mr. Jim Simms provided invaluable technical assistance in spectrometer modifications at M.I.T. Dr. Bertram Frenz of Texas A and M University provided help with computer programming for the permutational calculations. Dr. J. M. Read and Mr. D. Nickerson of duPont obtained the ^{19}F spectral data at 9.2 MHz. Dr. Paul Meakin of duPont pointed out an error in our original treatment of the intermolecular $\text{SF}_4 + \text{F}^-$ exchange calculations.

References and Notes

(1) Supported in part by Grants from the National Institutes of Health (GM 16020 and HL 15029, to G.M.W.), and by the National Science Founda-

- tion, (predoctoral fellowship to W.G.K. and Grant to E.L.M.).
- (2) (a) Department of Chemistry, Columbia University, New York, N.Y. 10027; (b) Cornell University; (c) Massachusetts Institute of Technology.
- (3) This structure has been verified for SF_4 in the gas phase by microwave spectroscopy and electron diffraction: (a) W. M. Tolles and W. D. Gwinn, *J. Chem. Phys.*, **36**, 1119 (1962); (b) K. Kimura and S. H. Bauer, *ibid.*, **39**, 3172 (1963). It may be viewed as an idealized trigonal bipyramid, if
- (4) F. A. Cotton, J. W. George, and J. S. Waugh, *J. Chem. Phys.*, **28**, 994 (1958).
- (5) E. L. Muetterties and W. D. Phillips, *J. Am. Chem. Soc.*, **81**, 1084 (1959).
- (6) E. L. Muetterties and W. D. Phillips, *J. Chem. Phys.*, **46**, 2861 (1967).
- (7) J. Bacon, R. J. Gillespie, and J. W. Quail, *Can. J. Chem.*, **41**, 1016 (1963).
- (8) J. A. Gibson, D. G. Ibbott, and A. F. Janzen, *Can. J. Chem.*, **51**, 3203 (1973).
- (9) R. L. Redington and C. V. Berney, *J. Chem. Phys.*, **43**, 2020 (1965); **46**, 2862 (1967).
- (10) R. A. Frey, R. L. Redington, and A. L. K. Aljibury, *J. Chem. Phys.*, **54**, 344 (1971). See also C. V. Berney, *J. Mol. Struct.*, **12**, 87 (1972).
- (11) W. Gombler and F. Seel, *J. Fluorine Chem.*, **4**, 333 (1974).
- (12) I. W. Levin and W. C. Harris, *J. Chem. Phys.*, **55**, 3048 (1971).
- (13) V. C. Ewing and L. E. Sutton, *Trans. Faraday Soc.*, **59**, 1241 (1963). See ref 3b for criticism of this work.
- (14) G. W. Chantry and V. C. Ewing, *Mol. Phys.*, **5**, 209 (1962).
- (15) B. J. Dalton, *Mol. Phys.*, **11**, 265 (1966).
- (16) W. G. Klemperer in "Dynamic Nuclear Magnetic Resonance Spectroscopy", F. A. Cotton and L. M. Jackman, Ed., Academic Press, New York, N.Y., 1975.
- (17) Intuitively, a reaction is symmetric if and only if transposition of axial fluorine atoms and equatorial fluorine atoms is symmetric in a reaction step. Formally, a reaction, h_i , is symmetric if and only if there exists a permutation p_k , which permutes all the equatorial sites with axial sites, and h_i and $h_j = p_k^{-1}h_i p_k$ are NMR nondifferentiable.
- (18) D. D. Gibler, C. J. Adams, M. Fischer, A. Zalkin, and N. Bartlett, *Inorg. Chem.*, **11**, 2325 (1972); M. Azeem, M. Brownstein, and R. J. Gillespie, *Can. J. Chem.*, **47**, 4159 (1969).
- (19) C. W. Tullock, D. D. Coffman, and E. L. Muetterties, *J. Am. Chem. Soc.*, **86**, 357 (1964); K. O. Christe, E. C. Curtis, C. J. Schack, and D. Pilipovich, *Inorg. Chem.*, **11**, 1679 (1972).
- (20) J. M. Williams and L. F. Schneemeyer, *J. Am. Chem. Soc.*, **95**, 5780 (1973).
- (21) Although this study provides support for the contention that the Berry rearrangement is the most common type of rearrangement observed for five-coordinate complexes, formally non-Berry types of rearrangement have been established for H_2PF_3 and Ph_2PF_3 : C. G. Moreland, G. O. Doak, and L. B. Littlefield, *J. Am. Chem. Soc.*, **95**, 255 (1973); J. W. Gilje, R. W. Braun, and A. H. Cowley, *J. Chem. Soc., Chem. Commun.*, **15** (1974). Pseudorotation of structurally complex five-coordinate compounds is complicated: G. M. Whitesides, M. Eisenhut, and W. M. Bunting, *J. Am. Chem. Soc.*, **96**, 5398 (1974); R. R. Holmes, *ibid.*, **96**, 4143 (1974).
- (22) W. A. Sheppard and D. W. Ovenall, *Org. Magn. Reson.*, **4**, 695 (1972).
- (23) D. H. Lehmer, *Amer. Math. Soc., Proc. Symp. Appl. Math.*, **10**, 179 (1958).
- (24) M. Eisenhut, H. L. Mitchell, D. D. Traficante, R. J. Kaufman, J. M. Deutch, and G. M. Whitesides, *J. Amer. Chem. Soc.*, **96**, 5385 (1974).
- (25) J. K. Krieger, J. M. Deutch, and G. M. Whitesides, *Inorg. Chem.*, **12**, 1535 (1973).
- (26) S. Alexander, *J. Chem. Phys.*, **37**, 967, 974 (1962); J. Kaplan, *ibid.*, **28**, 278 (1958); C. S. Johnson Jr., *Adv. Magn. Reson.*, **1**, 1 (1965), especially pp 53–56; J. I. Kaplan and G. Fraenkel, *J. Am. Chem. Soc.*, **94**, 2907 (1972).
- (27) P. Meakin, E. L. Muetterties, and J. P. Jesson, *J. Am. Chem. Soc.*, **94**, 5271 (1972); P. Meakin, E. L. Muetterties, F. N. Tebbe, and J. P. Jesson, *ibid.*, **93**, 4701 (1971).
- (28) The simplified equation used previously,²⁵ $I(\omega) \propto \text{Re}[\mathbf{I} \cdot \mathbf{A}^{-1} \cdot \mathbf{I}]$, where $\mathbf{I} = (\mathbf{I}^+)^2$ is a vector consisting of the intensities of the lines involved in the exchange, is clearly only useful when these lines have approximately equal intensities within each exchanging block.
- (29) H. S. Gutowsky, R. L. Vold, and E. J. Wells, *J. Chem. Phys.*, **43**, 4107 (1965).
- (30) P. Meakin and J. P. Jesson, *J. Am. Chem. Soc.*, **96**, 5751 (1974); J. P. Jesson and P. Meakin, *ibid.*, **96**, 5760 (1974).